7

A Computationally Efficient Numerical Simulation for Generating Atmospheric Optical Scintillations

Antonio Jurado-Navas, José María Garrido-Balsells,
Miguel Castillo-Vázquez and Antonio Puerta-Notario
Communications Engineering Department, University of Málaga
Campus de Teatinos
Málaga, Spain

1. Introduction

Atmospheric optical communication has been receiving considerable attention recently for use in high data rate wireless links (Juarez et al., 2006; Zhu & Kahn, 2002). Considering their narrow beamwidths and lack of licensing requirements as compared to microwave systems, atmospheric optical systems are appropriate candidates for secure, high data rate, cost-effective, wide bandwidth communications. Furthermore, atmospheric free space optical (FSO) communications are less susceptible to the radio interference than radio-wireless communications. Thus, FSO communication systems represent a promising alternative to solve the last mile problem, above all in densely populated urban areas. Then, applications that could benefit from optical communication systems are those that have platforms with limited weight and space, require very high data links and must operate in an environment where fiber optic links are not practical. Also, there has been a lot of interest over the years in the possibility of using optical transmitters for satellite communications (Nugent et al., 2009). This chapter is focused on how to model the propagation of laser beams through the atmosphere. In particular, it is concerned with line-of-sight propagation problems, i.e., the receiver is in full view of the transmitter. This concern is referred to situations where if there were no atmosphere and the waves were propagating in a vacuum, then the level of irradiance that a receiver would observe from the transmitter would be constant in time, with a value determined by the transmitter geometry plus vacuum diffraction effects. Nevertheless, propagation through the turbulent atmosphere involves situations where a laser beam is propagating through the clear atmosphere but where very small changes in the refractive index are present too. These small changes in refractive index, which are typically on the order of 10^{-6}, are related primarily to the small variations in temperature (on the order of 0.1-1°C), which are produced by the turbulent motion of the atmosphere. Clearly, fluctuations in pressure of the atmosphere also induces in refractive index irregularities. Thus, the introduction of the atmosphere between source and receiver, and its inherent random refractive index variations, can lead to power losses at the receiver and eventually it produces spatial and temporal fluctuations in the received irradiance, i.e. turbulence-induced signal power fading (Andrews & Phillips, 1998); but this random variations in atmospheric refractive index along the optical path also produces fluctuations in other wave parameters such as phase, angle of arrival and frequency. Such fluctuations can produce an increase in the

link error probability limiting the performance of communication systems. In this particular scenario, the turbulence-induced fading is called scintillation.
The goal of this chapter is to present an efficient computer simulation technique to derive these irradiance fluctuations for a propagating optical wave in a weakly inhomogeneous medium under the assumption that small-scale fluctuations are modulated by large-scale irradiance fluctuations of the wave.

2. Turbulence cascade theory

Temperature, pressure and humidity fluctuations, which are close related to wind velocity fluctuations, are primarily the cause of refractive index fluctuations transported by the turbulent motion of the atmosphere. In fact, all these effects let the formation of unstable air masses that, eventually, can be decomposed into turbulent eddies of different sizes, initiating the turbulent process. This atmospheric turbulent process can be physically described by Kolmogorov cascade theory (Andrews & Phillips, 1998; Brookner, 1970; Frisch, 1995; Tatarskii, 1971). Thus, turbulent air motion represents a set of eddies of various scales sizes. Large eddies become unstable due to very high Reynolds number and break apart (Frisch, 1995), so their energy is redistributed without loss to eddies of decreasing size until the kinetic energy of the flow is finally dissipated into heat by viscosity. The scale sizes of these eddies extend from a largest scale size L_0 to a smallest scale size l_0. Briefly, the largest scale size, L_0, is smaller than those at which turbulent energy is injected into a region. It defines an effective outer scale of turbulence which near the ground is roughly comparable with the height of the observation point above ground. On the contrary, the smallest scale size, l_0, denotes the inner scale of turbulence, the scale where the Reynolds number approaches unity and the energy is dissipated into heat. It is assumed that each eddy is homogeneous, although with a different index of refraction. These atmospheric index-of-refraction variations produce fluctuations in the irradiance of the transmitted optical beam, what is known as *atmospheric scintillation*.
It is widely accepted two further assumptions: the assumption of local homogeneity and the assumption of local isotropy. The first of them, the local homogeneity assumption, implies that the velocity difference statistics depend only on the displacement vector, $\mathbf{r}$. Hence, we may write the random variation of the refractive index as (Clifford & Strohbehn, 1970):

$$n(\mathbf{r}) = n_0 + n_1(\mathbf{r}), \tag{1}$$

where $\mathbf{r}$ is the displacement vector, $n_0 \cong 1$ is the ensemble average of n (its free space value), whereas $n_1(\mathbf{r}) \ll 1$ is a measure of the fluctuation of the refractive index from its free space value.
The second assumption is the supposition of local isotropy, which implies that only the magnitude of $\mathbf{r}$ is important. On the other hand, for locally homogeneous and isotropic turbulence, a method of analysis involving structure functions is successful in meeting such problem (Strohbehn, 1968). Hence, we can define the structure function for the refractive index fluctuations, $D_n(r)$, as:

$$D_n(r) = E\left[\left(n(\mathbf{r_1}) - n(\mathbf{r_1} + r)\right)^2\right] = 2\left[B_n(0) - B_n(r)\right], \tag{2}$$

where $E[\cdot]$ is the ensemble average operator, $B_n(r)$ is the covariance function of the refractive index and $r = |\mathbf{r}|$. By applying the Fourier transform to $B_n(r)$, we can obtain the spatial power spectrum of refractive index, $\Phi_n(\kappa)$. Then, we consider now that the outer scale, L_0, and the

inner scale, l_0, of turbulence satisfy the following conditions (Tatarskii, 1971) :

$$L_0 \gg \sqrt{(\lambda L)}, \quad \text{and} \quad l_0 \ll \sqrt{(\lambda L)}, \qquad [m], \tag{3}$$

where λ is the optical wavelength in meters and L is the transmission range, also expressed in meters. Hence, the result is the easiest of the expressions to describe $\Phi_n(\kappa)$, given by

$$\Phi_n(\kappa) = 0.033 C_n^2 \kappa^{-11/3}, \quad \frac{1}{L_0} \ll \kappa \ll \frac{1}{l_0}; \tag{4}$$

that it is usually named as *Kolmogorov spectrum* (Andrews & Phillips, 1998). This power spectrum of refractive index represents the energy distribution of turbulent eddies transported by the turbulent motion. In the last expression, κ is the spatial wave number and C_n^2 is the refractive-index structure parameter, which is altitude-dependent.

3. Wave propagation in random media

There is an extensive literature on the subject of the theory of line-of-sight propagation through the atmosphere (Andrews & Phillips, 1998; Andrews et al., 2000; Fante, 1975; Ishimaru, 1997; Strohbehn, 1978; Tatarskii, 1971). One of the most important works was developed by Tatarskii (Tatarskii, 1971). He supposed a plane wave that is incident upon the random medium (the atmosphere in this particular case). It is assumed that the atmosphere has zero conductivity and unit magnetic permeability and that the electromagnetic field has a sinusoidal time dependence (a monochromatic wave). Under these circumstances, Maxwell's equations take the form:

$$\nabla \cdot \mathbf{H} = 0, \tag{5}$$

$$\nabla \times \mathbf{E} = jk\mathbf{H}, \tag{6}$$

$$\nabla \times \mathbf{H} = -jkn^2\mathbf{E}, \tag{7}$$

$$\nabla \cdot (n^2\mathbf{E}) = 0; \tag{8}$$

where $j = \sqrt{-1}$, $k = 2\pi/\lambda$ is the wave number of the electromagnetic wave with λ being the optical wavelength; whereas $n(\mathbf{r})$ is the atmospheric index of refraction whose time variations have been suppressed and being a random function of position, $\mathbf{r}$. The ∇ operator is the well-known vector derivative $(\partial/\partial x, \partial/\partial y, \partial/\partial z)$. The quantities $\mathbf{E}$ and $\mathbf{H}$ are the vector amplitudes of the electric and magnetic fields and are a function of position alone. The assumed sinusoidal time dependence is contained in the wave number, k.
Thus, if we take the curl of Eq. (6) and, after substituting Eq. (7), then the following expression is obtained:

$$-\nabla^2\mathbf{E} + \nabla(\nabla \cdot \mathbf{E}) = k^2 n^2 \mathbf{E}, \tag{9}$$

where the ∇^2 operator is the Laplacian $(\partial^2/\partial x^2 + \partial^2/\partial y^2 + \partial^2/\partial z^2)$.
Equation (8) is expanded and solved for $\nabla \cdot \mathbf{E}$, and the result inserted into Eq. (9) so that we can obtain the final form of the vector wave equation:

$$\nabla^2\mathbf{E} + k^2 n^2(\mathbf{r})\mathbf{E} + 2\nabla\big(\mathbf{E} \cdot \nabla \log n(\mathbf{r})\big) = 0, \tag{10}$$

where $\mathbf{r} = (x, y, z)$ denotes a point in space. In Eq. (10) we have substituted the gradient of the natural logarithm for $\nabla n/n$. Equation (10) can be simplified by imposing certain characteristics of the propagation wave. In particular, since the wavelength λ for optical radiation is much smaller than the smallest scale of turbulence, l_0, (Strohbehn, 1968) the

maximum scattering angle is roughly $\lambda/l_0 \approx 10^{-4}$ rad. As a consequence, the last term on the left-hand side of Eq. (10) is negligible. Such a term is related to the change in polarization of the wave as it propagates (Strohbehn, 1971; Strohbehn & Clifford, 1967). This conclusion permit us to drop the last term, and Eq. (10) then simplifies to

$$\nabla^2 \mathbf{E} + k^2 n^2(\mathbf{r})\mathbf{E} = 0. \tag{11}$$

Because Eq. (11) is easily decomposed into three scalar equations, one for each component of the electric field, $\mathbf{E}$, we may solve one scalar equation and ignore the vector character of the wave until the final solution. Therefore if we let $U(\mathbf{r})$ denote one of the scalar components that is transverse to the direction of propagation along the positive x-axis (Andrews & Phillips, 1998), then Eq. (11) may be replaced by the scalar stochastic differential equation

$$\nabla^2 U + k^2 n^2(\mathbf{r})U = 0. \tag{12}$$

The index of refraction, $n(\mathbf{r}) = n_0 + n_1(\mathbf{r})$, fluctuates about the average value $n_0 = E[n(\mathbf{r})] \cong 1$, whereas $n_1(\mathbf{r}) \ll 1$ is the fluctuation of the refractive index from its free space value. Thus

$$\nabla^2 U + k^2 (n_0 + n_1(\mathbf{r}))^2 U = 0. \tag{13}$$

For weak fluctuation, it is necessary to obtain an approximate solution of Eq. (13) for small n_1. This can be done in two ways: one is to expand U in a series:

$$U = U_0 + U_1 + U_2 + ..., \tag{14}$$

and the other is to expand the exponent of U in a series:

$$U = \exp(\psi_0 + \psi_1 + \psi_2 + ...) = \exp(\psi). \tag{15}$$

In Eq. (14), U_0 is the unperturbed portion of the field in the absence of turbulence and the remaining terms represent first-order, second-order, etc., perturbations caused by the presence of random inhomogeneities. It is generally assumed that $|U_2(\mathbf{r})| \ll |U_1(\mathbf{r})| \ll |U_0(\mathbf{r})|$. In this sense, in Eq. (15), ψ_1, ψ_2 are the first-order and second-order complex phase perturbations, respectively, whereas ψ_0 is the phase of the optical wave in free space.

The expansion of Eq. (14) is the Born approximation, and has the important inconvenient that the complex Gaussian model for the field as predicted by this model does not compare well with experimental data. The other expansion given by Eq. (15) is called the Rytov solution. This technique is widely used in line-of-sight propagation problems because it simplifies the procedure of obtaining both amplitude and phase fluctuations and because its exponential representation is thought to represent a propagation wave better than the algebraic series representation of the Born method. From the Rytov solution, the wave equation becomes:

$$\nabla^2 \psi + (\nabla \psi)^2 + k^2 (n_0 + n_1(\mathbf{r}))^2 = 0. \tag{16}$$

This is a nonlinear first order differential equation for $\nabla\psi$ and is known as the Riccati equation. Consider now a first order perturbation, then

$$\psi(L, \mathbf{r}) = \psi_0(L, \mathbf{r}) + \psi_1(L, \mathbf{r}); \tag{17a}$$

$$n(\mathbf{r}) = n_0 + n_1(\mathbf{r}); \qquad n_0 \cong 1. \tag{17b}$$

Operating, assuming that $|\nabla\psi_1| \ll |\nabla\psi_0|$, due to $n_1(\mathbf{r}) \ll 1$, neglecting $n_1^2(\mathbf{r})$ in comparison to $2n_1(\mathbf{r})$, and equating the terms with the same order of perturbation, then the following expressions are obtained:

$$\nabla^2\psi_0 + (\nabla\psi_0)^2 + k^2 n_0^2(\mathbf{r}) = 0; \tag{18a}$$

$$\nabla^2\psi_1 + 2\nabla\psi_0\nabla\psi_1 + 2k^2 n_1(\mathbf{r}) = 0. \tag{18b}$$

The first one is the differential equation for $\nabla\psi$ in the absence of the fluctuation whereas turbulent atmosphere induced perturbation are found in the second expression. The resolution of Eq. (18) is detailed in (Fante, 1975; Ishimaru, 1997). For the particular case of a monochromatic optical plane wave propagating along the positive x-axis, i.e., $U_0(L, \mathbf{r}) = \exp(jkx)$, this solution can be written as:

$$\psi_1(L, \mathbf{r}) = \frac{k^2}{2\pi} \iiint_V n_1(\mathbf{r}') \frac{\exp\left(jk\left[|\mathbf{r} - \mathbf{r}'| - |L - x'|\right]\right)}{|\mathbf{r} - \mathbf{r}'|} d^3\mathbf{r}', \tag{19}$$

where the position $(L, \mathbf{r})$ denotes a position in the receiver plane (at $x = L$) whereas $(x', \mathbf{r}')$ represents any position at an arbitrary plane along the propagation path. The mathematical development needed to solve Eq. (19) can be consulted in (Andrews & Phillips, 1998; Ishimaru, 1997). Furthermore, the statistical nature of $\psi_1(L, \mathbf{r})$ can be deduced in an easy way. Equation (19) has the physical interpretation that the first-order Rytov perturbation, $\psi_1(L, \mathbf{r})$ is a sum of spherical waves generated at various points $\mathbf{r}'$ throughout the scattering volume V, the strength of each sum wave being proportional to the product of the unperturbed field term U_0 and the refractive-index perturbation, n_1, at the point $\mathbf{r}'$ (Andrews & Phillips, 1998). Thus it is possible to apply the central limit theorem. According to such a theorem, the distribution of a random variable which is a sum of N independent random variables approaches normal as $N \to \infty$ regardless of the distribution of each random variable. Application of the central limit theorem to this integral equation leads to the prediction of a normal probability distribution for ψ. Since we can substitute $\Psi = \chi + jS$, where χ and S are called the log-amplitude and phase, respectively, of the field, then application of the central limit theorem also leads to the prediction of a Gaussian (normal) probability distribution for both χ and S, at least up to first order corrections (χ_1 and S_1).

Accordingly, under this first-order Rytov approximation, the field of a propagating optical wave at distance L from the source is represented by:

$$U = \exp(\psi) = U_0(L, \mathbf{r}) \exp(\psi_1). \tag{20}$$

Hence, the irradiance of the random field shown in Eq. (20) takes the form:

$$I = |U_0(L, \mathbf{r})|^2 \exp(\psi_1 + \psi_1^*) = I_0 \exp(2\chi_1), \qquad [w/m^2] \tag{21}$$

where, from now onwards, we denote χ_1 as χ for simplicity in the notation. Hence,

$$I = I_0 \exp(2\chi), \qquad [w/m^2]. \tag{22}$$

In Eq. (21), operator $*$ denotes the complex conjugate, $|U_0|$ is the amplitude of the unperturbed field and I_0 is the level of irradiance fluctuation in the absence of air turbulence that ensures that the fading does not attenuate or amplify the average power, i.e., $E[I] = |U_0|^2$. This may be thought of as a conservation of energy consideration and requires the choice of $E[\chi] = -\sigma_\chi^2$, as was explained in (Fried, 1967; Strohbehn, 1978), where $E[\chi]$ is the ensemble average of

log-amplitude, whereas σ_χ^2 is its variance depending on the structure parameter, C_n^2. With all of these expressions, we have modeled the irradiance of the random field, I, in the space at a single instant in time. Now, because the state of the atmospheric turbulence varies with time, the intensity fluctuations will also be temporally correlated. Then, Eq. (22) can be expressed as:

$$I = \alpha_{sc}(t) \cdot I_0, \tag{23}$$

whereas $\alpha_{sc}(t) = \exp(2\chi(t))$ is the temporal behavior of the scintillation sequence and represents the effect of the intensity fluctuations on the transmitted signal. In Section 5.1.1, the space-to-time statistical conversion needed to derive Eq. (23) will be conveniently explained by assuming the well-known Taylor's hypothesis of frozen turbulence (Tatarskii, 1971; Taylor, 1938). The generation of this scintillation sequence is treated in detail further in this chapter.
As analyzed before, and by the central limit theorem, the marginal distribution of the log-amplitude, χ, is Gaussian. Thus,

$$f_\chi(\chi) = \left(\frac{1}{2\pi\sigma_\chi^2}\right)^{1/2} \exp\left[-\frac{(\chi - E[\chi])^2}{2\sigma_\chi^2}\right]. \tag{24}$$

Hence, from the Jacobian statistical transformation (Papoulis, 1991),

$$f_I(I) = \frac{f_\chi(\chi)}{|\frac{dI}{d\chi}|}, \tag{25}$$

the probability density function of the intensity, I, can be identified to have a lognormal distribution typical of weak turbulence regime. Then:

$$f_I(I) = \left(\frac{1}{2I}\right)\left(\frac{1}{2\pi\sigma_\chi^2}\right)^{1/2} \exp\left[-\frac{(\ln I - \ln I_0)^2}{8\sigma_\chi^2}\right]. \tag{26}$$

Theoretical and experimental studies of irradiance fluctuations generally center around the scintillation index. It was evaluated in (Mercier, 1962) and it is defined as the normalized variance of irradiance fluctuations:

$$\sigma_I^2 = \frac{E[I^2]}{\big(E[I]\big)^2} - 1. \tag{27}$$

With this parameter it is possible to define the weak turbulence regimes as those regimes for which the scintillation index given in Eq. (27) is less than unity. From the following property given in (Fried, 1966)

$$E\big[\exp(a \cdot g)\big] = \exp\left[aE[g] + \frac{1}{2}a^2 E\big[(g - E[g])^2\big]\right], \tag{28}$$

obeyed by any independent Gaussian random variable, g, with a being a constant, we can employ Eq. (28) to obtain the first and second order moments (mean value and variance, respectively) of the irradiance fluctuation. So,

$$E\big[I(\mathbf{r}, L)\big] = E\big[I_0(\mathbf{r}, L)\exp\big[(2\chi(\mathbf{r}, L)\big] = I_0(\mathbf{r}, L)\exp\big(2E[\chi(\mathbf{r}, L) + 2\sigma_\chi^2]\big), \tag{29}$$

where, as mentioned before, σ_χ^2 is the variance of log-amplitude of the scintillation. From energy-conservation consideration (Fried, 1967; Strohbehn, 1978), $E\big[I(\mathbf{r},L)\big] = I_0(\mathbf{r},L)$. Then, inserting this result into Eq. (29), we obtain:

$$E\big[\chi(\mathbf{r},L)\big] = -\sigma_\chi^2. \tag{30}$$

By repeating the same process to the root mean square of the irradiance, I, then:

$$E\big[I^2(\mathbf{r},L)\big] = E\big[\big(I_0(\mathbf{r},L)\exp\big[(2\chi(\mathbf{r},L)\big)^2\big] = I_0^2(\mathbf{r},L)\exp\big(4\sigma_\chi^2\big). \tag{31}$$

If we insert Eqs. (29)-(31) into Eq. (27), the scintillation index is finally derived as:

$$\sigma_I^2 = \frac{E[I^2]}{\big(E[I]\big)^2} - 1 = \exp\big(4\sigma_\chi^2\big) - 1 \cong 4\sigma_\chi^2 \quad \text{if} \quad \sigma_I^2 \ll 1, \tag{32}$$

depending on σ_χ^2. It can be seen (Andrews & Phillips, 1998; Andrews et al., 2001), that the derived expression for the scintillation index is proportional to the Rytov variance for a plane wave given by:

$$\sigma_1^2 = 1.23 C_n^2 k^{7/6} L^{11/6}, \tag{33}$$

where, again, C_n^2 ($\mathrm{m}^{-2/3}$) is the index of refraction structure parameter, $k = 2\pi/\lambda$ (m^{-1}) is the optical wave number, λ (m) is the wavelength, and L (m) is the propagation path length between transmitter and receiver. The Rytov variance represents the scintillation index of an unbounded plane wave in weak fluctuations based on a Kolmogorov spectrum as the shown in Eq. (4), but is otherwise considered a measure of optical turbulence strength (Andrews et al., 2001).

4. Generation of scintillation sequences

Any kind of mechanism to model the behavior of the turbulent atmosphere as a time-varying channel is necessary. Let the transmitted instantaneous optical power signal defined by

$$s(t) = \sum_i a_i \cdot P_{peak} \cdot p_n(t - iT_b) \qquad i \in \mathbf{Z} \tag{34}$$

where the random variable a_i takes the values of 0 for the bit "0" (off pulse) and 1 for the bit "1" (on pulse), P_{peak} the peak optical power transmitted each bit period, T_b, with active pulse; and $p_n(t)$ is the pulse shape having normalized amplitude. In this manner, the received signal will consist, in a generic channel, of two terms: the first one is the line-of-sight (LOS) contribution, and the second one is due to energy which is scattered to the receiver. This fact will be thought as a multipath channel. Every contribution (the LOS component and each multipath contribution) will travel through different paths in the atmosphere, each of them with a different propagation delay, $\tau_n(t)$. Thus, the expression for the received signal can be written as:

$$y(t) = \sum_n \alpha_{sc_n}(t) s(t - \tau_n(t)), \tag{35}$$

where $\alpha_{sc_n}(t)$ is the time-varying scintillation sequence representing the effect of the intensity fluctuations on the nth-multipath component. As discussed in (Fante, 1975; Ishimaru, 1997; Kennedy, 1968), dispersion and beam spreading due to turbulent atmosphere can be neglected. Only for the very short pulses less than 100 ps proposed for high-data rate

communications systems, or in extreme scenarios such as the one detailed in (Ruike et al., 2007), where sand and dust particles are likely present, pulse spreading owing to turbulent atmosphere must be included. For this latter case, physically, two possible causes exist for this pulse spreading: scattering (dispersion) and pulse wander (fluctuations in arrival time), although it is found that, under the condition of weak scattering, pulse wandering dominates the contribution to the overall broadening of the pulse (Jurado-Navas et al., 2009; Young et al., 1998).

Nonetheless, a general scenario where dispersion and beam spreading can be neglected is assumed in this chapter. Hence, the channel impulse response, $h(\tau_n;t)$, can be obtained by substituting $s(t)=\delta(t)$ into Eq. (35). Then,

$$h(\tau_n;t)=\sum_n \alpha_{sc_n}(t)\delta(t-\tau_n(t)). \tag{36}$$

Some channel models assume a continuum of multipath delays, in which case the sum in Eq. (36) becomes an integral which simplifies to a time-varying complex amplitude associated with each multipath delay, τ, as indicated in (Goldsmith, 2005):

$$h(\tau;t)=\int \alpha_{sc}(\xi;t)\delta(\tau-\xi)d\xi=\alpha_{sc}(\tau;t), \tag{37}$$

by using the definition of the Dirac delta function, $\delta(t)$. Note that $h(\tau;t)$ has two time parameters: the time t when the impulse response is observed at the receiver, and the time $t-\tau$ when the impulse is launched into the channel relative to the observation time, t. Hence, $h(\tau;t)$ is the response of the system to a unit impulse applied at time t.

An important characteristic of a multipath channel is the time delay spread, T_m, it causes to the received signal. This delay spread equals the time delay between the arrival of the first received signal component (LOS or multipath) and the last received signal component associated with a single transmitted pulse. In these atmospheric optical communication systems, the delay spread is small compared to the inverse of the signal bandwidth, as commented above, then there is little time spreading in the received signal. Of course, the propagation delay associated with the i-th multipath component is $\tau_i \leq T_m \nVdash i$ so that $s(t-\tau_i)\approx s(t) \nVdash i$, and then, Eq. (35) can be expressed as:

$$y(t)=s(t)\sum_n \alpha_{sc_n}(t). \tag{38}$$

As the propagation delay is very small, then the corresponding multipath scintillation sequences will be received in the same bit interval and having the same magnitude. Finally,

$$y(t)=s(t)\alpha_{sc}(t). \tag{39}$$

Then, the received light intensity is compounded of the transmitted instantaneous optical power signal, $s(t)$, initially transmitted, and affected in a multiplicative manner by the scintillation sequence, $\alpha_{sc}(t)$. This latter one represents the intensity fluctuations due to the effect of the atmospheric turbulence on the transmitted signal, $s(t)$.

Finally, a characteristic of $\alpha_{sc}(t)$ is its time-varying nature. This time variation arises from the turbulent motion of the atmosphere described by Kolmogorov cascade theory (Tatarskii, 1971). The component of the wind velocity transverse to the propagation direction, $u_\perp$, characterizes the average fade duration.

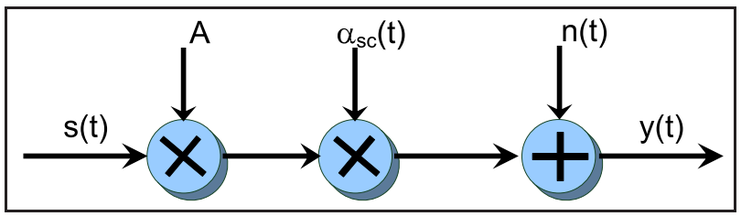

Fig. 1. Scheme model of the turbulent atmospheric optical model.

Obviously, the lognormal atmospheric channel model employed in the previous section and represented by Eqs. (22)-(23) is consistent with Eq. (39) derived here. Hence, the atmospheric channel model must be consisted of a multiplicative noise model that enhances the effect of the atmospheric turbulence on the propagation of the transmitted optical signal. Clearly, accordingly to Eqs. (22)-(23) and Eq. (39), an appropriate channel model for describing these effects is shown in Fig. 1. This scalar model assumes the transmitted field to be linearly polarized (no polarization modulation). This fact is realistic because the depolarization effects of the atmospheric turbulence are negligible (Strohbehn, 1968; 1971; Strohbehn & Clifford, 1967) and because it is reasonable to assume that the relevant noise has statistically independent polarization components (Kennedy, 1968).
In Fig. 1 the real process $s(t)$ represents the instantaneous optical power transmitted, and given by Eq. (34). The additive white Gaussian noise is represented by $n(t)$ and it is assumed to include any shot noise caused by ambient light that may be much stronger than the desired signal as well as any front-end receiver thermal noise in the electronics following the photodetector. On the other hand, the factor A involves any weather-induced attenuation caused by rain, snow, and fog that can also degrade the performance of atmospheric optical communication systems in the way shown in (Al Naboulsi & Sizun, 2004; Muhammad et al., 2005), but it is not considered in this chapter ($A = 1$). Finally, the process $\alpha_{sc}(t) = \exp(2\chi(t))$ denotes the temporal behavior of the scintillation sequence and represents the effect of the intensity fluctuations on the transmitted signal, in the same way as Eq. (39) or Eq. (23).

5. Turbulent atmospheric channel model

The goal of this section is to obtain the time-varying scintillation sequence, denoted as $\alpha_{sc}(t)$ in Fig. 1, that represents the fluctuations of the intensity on the transmitted signal owing to the adverse effect of the turbulent atmosphere. To achieve this purpose, we start with the channel model proposed in (Jurado-Navas et al., 2007). Thus, to generate the $\alpha_{sc}(t)$ coefficients, a scheme based on Clarke's method (Rappaport, 1996) is implemented.
In brief, Clarke's model is based on a low-pass filtering of a random Gaussian signal, $z(t)$, as it is shown in Fig. 2. Hence, the output signal, $\chi(t)$, keeps on being statistically Gaussian, but shaped in its power spectral density by the $H_{sc}(f)$ filter. The output signal, $\chi(t)$, is the log-amplitude perturbation of the transmitted optical wave, as explained in previous sections. Next, $\chi(t)$ is passed through a nonlinear device which converts its probability distribution from Gaussian to lognormal, according to Eq. (26), typical of a weak turbulence regime, the scenario that has been considered through this chapter.

5.1 Covariance function: weak fluctuations

The first task we need to achieve is to obtain the shape of the filtering stage displayed in Fig. 2. In this respect, the theoretical Kolmogorov theory requires to solve the following expression

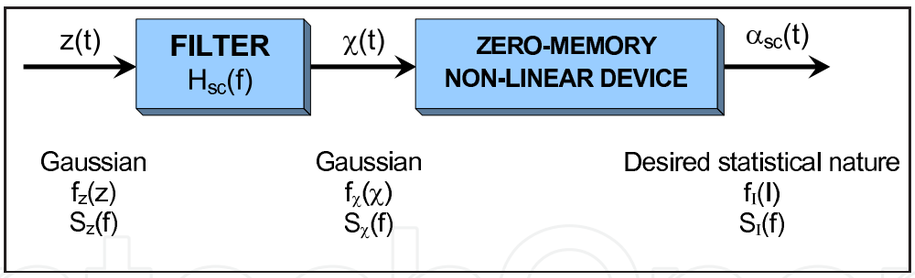

Fig. 2. Block diagram to generate the scintillation sequence, $\alpha_{sc}(t)$.

for the covariance function for irradiance fluctuations, $B_I(r, L)$:

$$B_I(r,L) = 8\pi^2 k^2 L \int_0^1 \int_0^\infty \kappa \Phi_n(\kappa) J_0(\kappa r) \left(1 - \cos \frac{L\kappa^2 \xi}{k}\right) d\kappa d\xi, \tag{40}$$

where κ is the spatial wave number, $\Phi_n(\kappa)$ denotes the spatial power spectrum of refractive index, k is the wave number, L represents the propagation path length whereas $J_0(\cdot)$ is the Bessel function of the first kind and 0th order. In Eq. (40), an homogeneous and isotropic random medium has been assumed in addition to a conversion to cylindrical coordinates since B_I is a function of the transverse distance r (Ishimaru, 1997; Tatarskii, 1971). The obtention of such an expression is conveniently treated in (Ishimaru, 1997; Lawrence & Strohbehn, 1970) and will be the starting point to generate the filter $H_{sc}(f)$. Nevertheless, Eq. (40) requires a high computational complexity when any theoretical model for the spatial power spectrum of refractive index, $\Phi_n(\kappa)$, is employed. This feature is a critical point; in this respect, we develop an efficient approximation to calculate such an integration that will be detailed below in Subsection 5.1.2. Anyway, and by the Wiener-Khintchine theorem, we can obtain the resulting temporal spectrum of irradiance fluctuations from which the filter frequency response, $H_{sc}(f)$, is obtained.

5.1.1 Taylor's hypothesis of frozen turbulence

A useful property in turbulent media is the well-known Taylor's hypothesis of frozen turbulence (Jurado-Navas & Puerta-Notario, 2009; Tatarskii, 1971; Taylor, 1938). Modeling the movement of atmospheric eddies is extremely difficult and a simplified "frozen air" model is normally employed. Thus under this hypothesis, the collection of atmospheric eddies will remain frozen in relation to one another, while the entire collection is transported as a whole along some direction by the wind. When a narrow beam propagating over a long distance is assumed, the refractive index fluctuations along the direction of propagation will be well-averaged and will be weaker than those along the transverse direction to propagation. Hence, consider the case when the atmospheric inhomogeneities move at constant velocity, $u_\perp$, perpendicular to the propagation direction. Taylor's frozen-in hypothesis can be expressed as (Lawrence & Strohbehn, 1970):

$$n(\mathbf{r}, t+\tau) = n(\mathbf{r} - u_\perp \tau, t). \tag{41}$$

Accordingly, a space-to-time conversion of statistics can be accomplished assuming the use of Taylor's hypothesis. The turbulence correlation time is therefore

$$\tau_0 = \frac{d_0}{u_\perp}, \qquad [s]; \tag{42}$$

where d_0 is the correlation length of intensity fluctuations. When the propagation length, L satisfies the condition $l_0 < \sqrt{\lambda L} < L_0$, with λ being the optical wavelength and with l_0 and L_0 being the inner and outer scale of turbulence, respectively, then d_0 can be approximated by (Andrews & Phillips, 1998; Tatarskii, 1971)

$$d_0 \approx \sqrt{\lambda L}, \qquad [m]. \tag{43}$$

5.1.2 Shaping a Gaussian temporary spectrum of irradiance

As explained at the begining of this subsection, to obtain the filter frequency response, $H_{sc}(f)$, needed to generate the time-varying nature of scintillation sequence, $\alpha_{sc}(t)$, (see Fig. 2), the covariance function of irradiance fluctuations, B_I, must be employed. Under the assumption of weak irradiance fluctuations ($\sigma_\chi^2 \ll 1$), the covariance functions of I and χ are related by $B_I(r) \simeq 4B_\chi(r)$, in a similar reasoning to obtain Eq. (32), where r denotes separation distance between two points on the wavefront. Taking this latter relationship into account, the filter, $H_{sc}(f)$, employed in the scheme and displayed in Fig. 2 corresponds, for simplicity, to the log-amplitude fluctuations. Furthermore, based on the Taylor frozen turbulence hypothesis, spatial statistics can be converted to temporal statistics by knowledge of the average wind speed transverse to the direction of propagation. In the case of a plane wave, this is accomplished by setting $r = u_\perp \tau$, where $u_\perp$ is the wind velocity transverse to the propagation direction in meters per second, and τ is in seconds. Now, taking into account an approximation developed by Andrews and Phillips (Andrews & Phillips, 1998), Eq. (40), in the case of a plane wave, reduces to

$$B_I(\tau, L) = 3.87\sigma_1^2 \mathrm{Re}\left[j^{5/6}\, {}_1F_1\left(-\frac{5}{6}; 1; \frac{jk(u_\perp \tau)^2}{2L}\right) - 0.60\left(\frac{k(u_\perp \tau)^2}{L}\right)^{5/6}\right], \tag{44}$$

with ${}_1F_1(a;b;v)$ being the confluent hypergeometric function of the first kind whereas σ_1^2 is the Rytov variance for a plane wave, as expressed in Eq. (33) that, under weak fluctuation, can also be written as $\sigma_1^2 \cong \sigma_I^2$. Even so, Eq. (44) still suffers from significant numerical complexity, especially if we try to solve the power spectral density (PSD), so an easier approach is proposed by the authors in (Jurado-Navas et al., 2007). Hence, suppose small separation distances in Eq. (44) so that $l_0 \ll r \ll \sqrt{\lambda L}$, and assume $B_I(r) \simeq 4B_\chi(r)$. Now, if we consider the following approximation for the hypergeometric function:

$${}_1F_1(a;b;-v) \approx 1 - \frac{av}{b} \qquad |v| \ll 1; \tag{45}$$

then

$$R_\chi(\tau) = E[\chi(t)\chi^*(t-\tau)] = \sigma_\chi^2 \exp\left[-\left(\frac{\tau}{\tau_0}\right)^2\right] = B_\chi(u_\perp \tau), \tag{46}$$

where $R_\chi(\tau)$ is the autocorrelation function of the process $\chi(t)$. We must remark that, in Eq. (46), it has been assumed a weak fluctuation regime so that we can state that $(E[\chi])^2 = \sigma_\chi^4 \approx 0$. Thus $R_\chi(\tau) \cong B_\chi(\tau)$, with $B_\chi(\tau)$ being the covariance function of the log-amplitude perturbation.

5.2 Design of the filter frequency response

From Eq. (46), the resulting temporal spectrum of log-amplitude perturbation, $\chi(t)$, can be obtained (Ishimaru, 1997; Tatarskii, 1971) as:

$$S_\chi(f) = 4\int_0^\infty B_\chi(\tau)\cos 2\pi f\tau d\tau. \tag{47}$$

Since assumed a weak irradiance fluctuations regime, $R_\chi(\tau) \cong B_\chi(\tau)$ so that we can apply the Wiener-Khintchine theorem to solve Eq. (47). Thus the power spectral density of χ is given by:

$$|H_{sc}(f)|^2 = \int_{-\infty}^{\infty} R_\chi(\tau)\exp\left(-j2\pi f\tau\right)d\tau = \sigma_\chi^2\tau_0\sqrt{\pi}\exp\left[-\left(\pi\tau_0 f\right)^2\right]. \tag{48}$$

To corroborate the Gaussian approximation regarding to the theoretical zero inner-scale ($l_0 = 0$) Kolmogorov spectrum, both of them have been plotted in Figure 3 with a remarkable resemblance between them. As an interesting feature, the Kolmogorov spectrum was obtained after substitution Eq. (4) into Eq. (48).

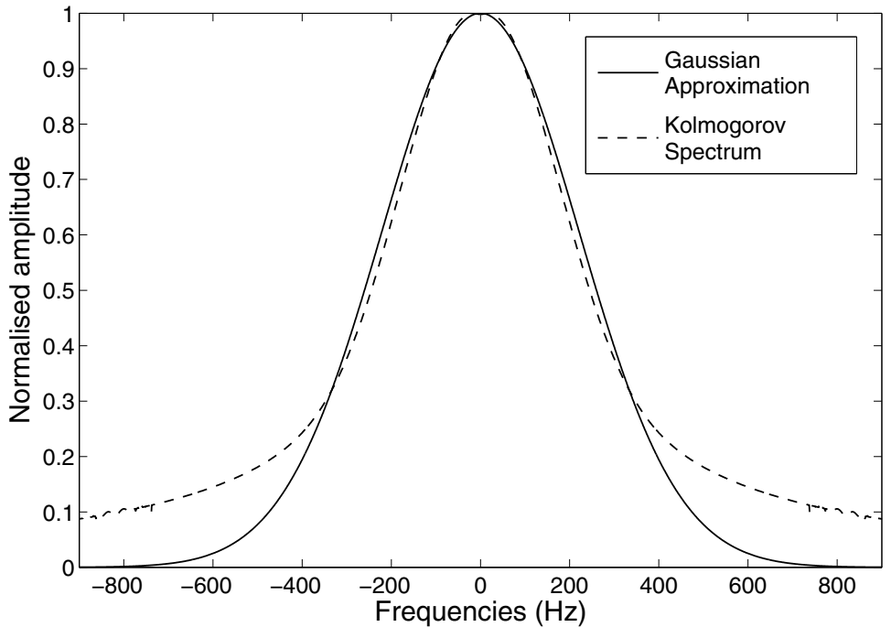

Fig. 3. Zero inner-scale model of Kolmogorov spectrum (Andrews et al., 2001) against Gaussian approximation conformed spectrum (Jurado-Navas et al., 2007).

To obtain the filter $H_{sc}(f)$, we assume a causal channel. This fact is desirable and so, the output sequence value of the system at the instant time $t = t_0$ depends only on the input sequence values for $t \leq t_0$. This implies that the system is nonanticipative (Oppenheim, 1999). Thus if the system is causal, zero phase is not attainable, and consequently, some phase distortion must be allowed. To design the nature of the filter phase it is sufficient to mention two concepts: first, a nonlinear phase can have an important effect on the shape of a filtered signal, even when the frequency-response magnitude is constant; and second, the effect of linear phase with integer slope is a simple time shift. It seems to be desirable to design systems to have exactly or approximately linear phase owing to the hard effort made to obtain the modulus of the filter.

Hence the filter frequency response is designed to have a linear phase:

$$H_{sc}(f) = |H_{sc}(f)| \exp(-j2\pi f\alpha), \tag{49}$$

where α is the delay introduced by the system. The magnitude of α will be established to half the length, M, of the filter impulse response, $H_{sc}(f)$. Consequently, the final expression for the behavior of the filter included in Figure 2 is:

$$H_{sc}(f) = \left(\sigma_\chi^2 \tau_0 \sqrt{\pi}\right)^{1/2} \exp\left[-\frac{1}{2}(\pi\tau_0 f)^2\right] \exp\left[-j2\pi f\alpha\right]. \tag{50}$$

The procedure to accomplish from now onwards is the following: for the time domain method, we first determine the impulse response of the filter, $h_{sc}(t) = \mathfrak{F}^{-1}\{H_{sc}(f)\}$, but represented in its discrete-time version: $h_{sc}[n], 0 \leq k \leq M-1$, with M being the length of the filter impulse, whereas $\mathfrak{F}^{-1}\{\cdot\}$ is the inverse Fourier transform operator. In this respect, we initially select a sampling rate, F_s, that is five times the maximum bandwidth of the filter which is proportional to the inverse of the turbulence correlation time, τ_0, such that:

$$F_s\tau_0 \approx 5. \tag{51}$$

Ultimately, the scintillation will be interpolated up to a much higher sample rate as will be discussed subsequently. This fact let us achieve a great reduction of computational load. We denote $\hat{\chi}[n]$ as the discrete output sequence value of the filter at a frequency rate of $F_s = 5/\tau_0$ whereas $\chi[n]$ represents the discrete log-amplitude scintillation with the proper bandwidth for its power spectral density, as a consequence of the interpolation process that fills in the missing samples of $\hat{\chi}[n]$.

5.3 Continuous-to-discrete time conversion

At this point, and as just commented, it is necessary to sample the continuous-time signal of the filter converting it in a discrete time signal because of their advantages in realizations. Hence we will obtain $\alpha_{sc}[n]$.

The chosen sampling frequency is F_s inversely proportional to the turbulence correlation time, τ_0. We initially choose $F_s\tau_0 \approx 2-5$, depending on the computer's memory. This initial value is not very relevant since the scintillation sequence will be interpolated later up to a much higher sample rate. However, this fact let the discrete Fourier transform (DFT) computation time be remarkably reduced. The election of the F_s magnitude must satisfy the Nyquist sampling theorem and should help avoid aliasing, should improve resolution and should reduce noise, removing the possibility of obtaining a very oversampled signal with very few useful samples of information (Oppenheim, 1999).

The $N-$point discrete version of the filter, denoted by $H_{sc}[k]$, is given by

$$\begin{aligned} H_{sc}[k] = H_{sc}(e^{j\omega}), \qquad & 0 \leq k \leq N-1, \\ & \omega = \frac{2\pi k}{N}; \end{aligned} \tag{52}$$

where it is employed a $N-$point DFT, with ω being the discrete frequency in rads. In Eq. (52), $H_{sc}(e^{j\omega})$ is the Fourier transform of $h_{sc}[n]$, being this latter one the sequence of samples of the continuous-time impulse response $h_{sc}(t)$, whereas $H_{sc}[k]$ is obtained by sampling $H_{sc}(e^{j\omega})$ at frequencies $\omega_k = \frac{2\pi k}{N}$. Consequently, from (Oppenheim, 1999), and substituting Eq. (50) into

Eq. (52):

$$H_{sc}[k] = F_s\left(\sigma_\chi^2 \tau_0 \sqrt{\pi}\right)^{1/2} \exp\left[-\frac{1}{2}\left(\pi \tau_0 \frac{kF_s}{N}\right)^2\right] \exp\left[-j2\pi \frac{M}{2}\frac{kF_s}{N}\right], \qquad 0 \leq k \leq N/2. \tag{53}$$

Since the desired impulse response, $h_{sc}[k]$ $0 \leq k \leq M-1$, is a real sequence, by applying the Hermitian symmetry property it follows that

$$\begin{aligned} H_{sc}[k] &= H_{sc}(e^{j\omega}), \quad 0 \leq k \leq N/2, \quad \omega = \frac{2\pi k}{N}; \\ H_{sc}[N-k] &= H_{sc}^*[k], \quad 1 \leq k \leq N/2 - 1. \end{aligned} \tag{54}$$

By applying the inverse-DFT (IDFT) of $H_{sc}[k]$, we can obtain $h_{sc}[n] = \mathfrak{F}^{-1}\{H_{sc}[k]\}$. Consider $h_{sc}[n]$ as a finite-length sequence, i.e. a finite impulse response (FIR) system. Accordingly, one of the simplest method of FIR filter design is called the *window method*, explained in (Oppenheim, 1999). The method consists in defining a new system with impulse response $h_{wsc}[n]$. This impulse response is the desired causal FIR filter given by

$$h_{wsc}[n] = \begin{cases} h_{sc}[n]w[n], & 0 \leq n \leq M, \\ 0, & \text{otherwise.} \end{cases} \tag{55}$$

In Eq. (55), $w[n]$ is the finite-duration window. In this paper, we use a M-points Hamming window symmetric about the point $M/2$ of the form

$$w[n] = \begin{cases} 0.54 - 0.46\cos(2\pi n/M), & 0 \leq n \leq M, \\ 0, & \text{otherwise;} \end{cases} \tag{56}$$

owing to it is optimized to minimize the maximum (nearest) side lobe. As a result, the definitive expression for $h_{wsc}[n]$ is:

$$h_{wsc}[n] = \frac{1}{N} w[n] \sum_{k=0}^{N-1} H_{sc}[k] \exp\left\{j\frac{2\pi kn}{N}\right\}, \qquad 0 \leq n \leq M-1. \tag{57}$$

Consequently, the output sequence without being upsampled, $\hat{\chi}[n]$, accomplished with the filter stage of Fig. 2, is of the form:

$$\hat{\chi}[n] = \beta \sum_{k=0}^{M-1} h_{wsc}[k] z[n-k], \tag{58}$$

where β is the scaling constant chosen to yield the desired output variance, σ_χ^2, with $z[n]$ representing the discrete version of $z(t)$, this latter being a random unit variance Gaussian input signal to be filtered by $H_{sc}(f)$, as it is shown in Figure 2. We must remind that $\hat{\chi}[n]$ is a Gaussian version of the scintillation sequence without being upsampled, i.e., at $F_s = 5/\tau_0$, whereas $\chi[n]$ is the upsampled and accuracy version of $\hat{\chi}[n]$.

Equation (58), however, makes reference to a linear convolution between two finite-duration sequences: $h_{wsc}[n]$, M samples in extent; and $z[n]$, N samples in extent. Since we want the product to represent the DFT of the linear convolution of $h_{wsc}[n]$ and $z[n]$, which has length $M+N-1$, the DFTs that we compute must also be at least that length, i.e., both $h_{wsc}[n]$ and $z[n]$ must be augmented with sequence values of zero amplitude. This process is referred to

as zero-padding (Oppenheim, 1999) and it is necessary to adopt it to compute such a linear convolution by a circular convolution avoiding time-aliasing of the first $M-1$ samples. With the purpose of employing fast Fourier transform (FFT) algorithms to compute all values of the DFTs, it is required that we first zero-pad N samples of the white, unit variance random Gaussian input sequence $z[n]$ and M samples of $h_{wsc}[n]$ out to $2N$ samples and compute the FFT of each (zero-padded) sequence. As an interesting remark, for the computation of all N values of a DFT using the definition, the number of arithmetical operations required is approximately N^2, while the amount of computation is approximately proportional to $N\log_2 N$ for the same result to be computed by an FFT algorithm (Oppenheim, 1999). Even more, when N is a power of 2, the well-known decimation-in-time radix-2 Cooley-Tukey algorithm can be employed and then, the computational load is reduced to only $(N/2)\log_2 N$. Such an algorithm is based on a divide and conquer technique by breaking a length-N DFT into two length-N/2 DFTs followed by a combining stage consisting of many size-2 DFTs called "butterfly" operations, so-called because of the shape of the data-flow diagrams (Oppenheim, 1999). Thus, according to these criteria, the zero-pad versions of $z[n]$ and $h_{wsc}[n]$, denoted as $z_{zp}[n]$ and $h_{wsc;zp}[n]$ respectively, are:

$$z_{zp}[n] = \begin{cases} z[n], & 0 \leq n \leq N-1, \\ 0, & N \leq n \leq 2N-1; \end{cases} \tag{59}$$

and

$$h_{wsc;zp}[n] = \begin{cases} h_{wsc}[n], & 0 \leq n \leq M-1, \\ 0, & M \leq n \leq 2N-1. \end{cases} \tag{60}$$

Hence, after computing an FFT of length $2N$ to the sequences written in Eqs. (59)-(60), we can obtain the following expressions:

$$Z_{zp}[k] = \sum_{n=0}^{2N-1} z_{zp}[n] e^{-j2\pi kn/(2N)}, \tag{61}$$

and

$$H_{wsc;zp}[k] = \sum_{n=0}^{2N-1} h_{wsc;zp}[n] e^{-j2\pi kn/(2N)}. \tag{62}$$

Now, the inverse FFT of the product, $Z_{zp}[k] \cdot H_{wsc;zp}[k]$ is then computed and the first N samples of the result are retained, i.e.

$$\hat{\chi}[n] = \frac{1}{2N} \sum_{k=0}^{2N-1} Z_{zp}[k] H_{wsc;zp}[k] e^{j2\pi kn/(2N)}, \quad 0 \leq n \leq N-1, \tag{63}$$

Thus, once this latter expression were multiplied by the scaling constant, β, the result will coincide with the first N samples of the linear convolution between $h_{wsc}[n]$ and $z[n]$.

5.4 Increasing the sampling rate

Up until now, the temporal behavior of a Gaussian-amplitude scintillation sequence was modeled. Nevertheless, this sequence lacks the right value of the temporal frequency of the amplitude and, consequently, its adequate temporal variability. Such a temporal frequency will be achieved including the frequency content of the intensity fluctuation power spectral density. Fante, in (Fante, 1975), observed that the power spectral density bandwidth of the

intensity fluctuations under weak turbulence is:

$$f_c = \frac{1}{\tau_0} = \frac{u_\perp}{\sqrt{\lambda L}}, \tag{64}$$

as a direct result of the atmospheric motion, with λ being the optical wavelength, L is the propagation path length and $u_\perp$ denotes the wind velocity transverse to the propagation direction. By including this bandwidth reported in Eq. (64), we will be able to increase the sampling rate by a factor of P. The way of yielding this is:

$$\begin{cases} F_s = \frac{i}{\tau_0} = i \cdot f_c, & i \in [2-5] \\ P = \frac{R}{F_s}; \end{cases} \tag{65}$$

where R is the desired bit rate in bits/s; and F_s is the sampling frequency. Thus, and found P, the output samples of the filter H_{sc}, are upsampled by linear interpolation:

$$\chi[n] = \hat{\chi}[i] + \left\{\hat{\chi}[i+1] - \hat{\chi}[i]\right\}\left(\frac{n - i \cdot P}{P}\right), \text{ if } \text{i·P} \leq \text{n} \leq \text{(i+1)·P–1}, \quad 0 \leq \text{i} \leq \text{N–1}; \tag{66}$$

where, as we said before, $\chi[n]$ is the upsampled version of $\hat{\chi}[n]$ shown in Eq. (58).

5.5 Changing the statistical description

At this point, we have modeled the known random log-amplitude of the scintillation, χ, with a statistically Gaussian PDF, $f_\chi(\chi)$. Next, its PDF is converted from Gaussian to a lognormally distributed one that is generally accepted for the irradiance fluctuations, I, under weak turbulence conditions; or to a gamma-gamma PDF, a K PDF or even a Beckmann probability density (Hill & Frehlich, 1997) that much more accurately reflects the statistics of the intensity scintillations if Rytov variance (Andrews & Phillips, 1998) increases even beyond the limits of the weak turbulence regime. The resulting PDF is here denoted as $f_{\alpha_{sc}}(\alpha_{sc})$.

The statistical conversion is carried out with the zero-memory nonlinear device that was shown in Fig. 2. According to (Gujar & Kavanagh, 1968), this nonlinear device is just a one-to-one transformation between χ and α_{sc} of the form:

$$f_\chi\left(\chi - \frac{\delta\chi}{2}\right)|\delta\chi| = f_{\alpha_{sc}}\left(\alpha_{sc} - \frac{\delta\alpha_{sc}}{2}\right)|\delta\alpha_{sc}|, \tag{67}$$

where $f_{\alpha_{sc}}(\alpha_{sc})$ is the PDF typical of the scintillation coefficients sequence (lognormal, gamma-gamma or Beckmann, for instance). This $f_{\alpha_{sc}}(\alpha_{sc})$ PDF is identical to the probability density function of the irradiance fluctuations, I. Consequently, for any point (χ, α_{sc}) in the transformation, the probability of $\chi(t)$ being in the range $(\chi - \delta\chi)$ to χ is equal to the probability that $\alpha_{sc}(t)$ is in the corresponding range of $(\alpha_{sc} - \delta\alpha_{sc})$ to α_{sc}, where $\delta\chi$ and $\delta\alpha_{sc}$ are small increments beyond the points of study (χ_0, α_{sc_0}) in every moment. The known initial points are given by the mean values of the sequences χ and I, whose values are given by (Huang et al., 1993; Zhu & Kahn, 2002):

$$\begin{aligned} \chi_0 &= -\sigma_\chi^2, \\ E[I] &\equiv \alpha_{sc_0}; \end{aligned} \tag{68}$$

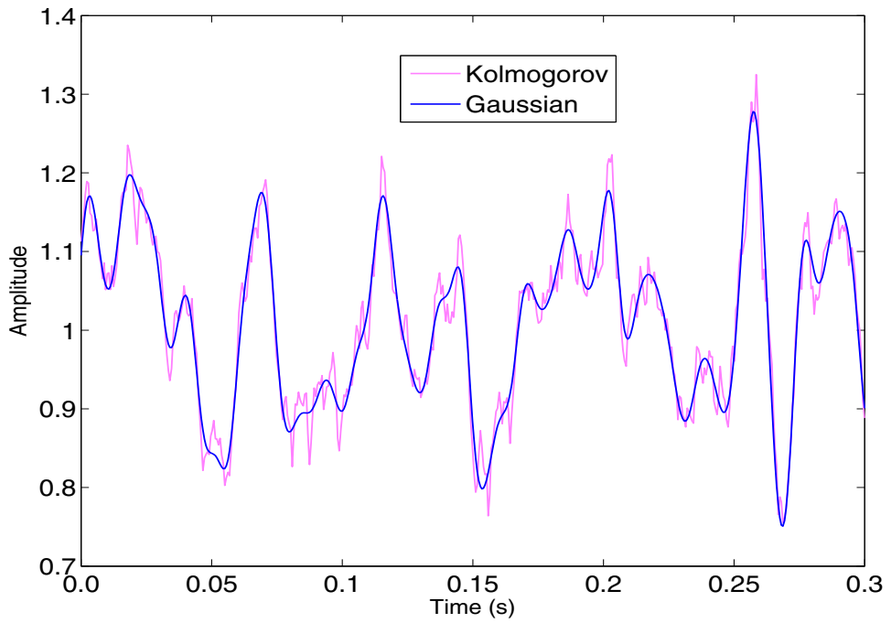

Fig. 4. Comparison of time series realizations characterized by the Kolmogorov (magenta) and Gaussian (blue) spectra.

where $E[\cdot]$ denotes an ensemble average or, equivalently with the assumption of ergodicity, a long-time average; and σ_I^2 is the normalized irradiance variance.
To illustrate the effect of a Gaussian spectrum, Figure 4 shows segments of time series realizations generated by the process of filtering white Gaussian noise with the proposed Gaussian spectrum given in Eq. (48). This realization is compared with another obtained by using the theoretical Kolmogorov spectrum.

6. Numerical results

To study the performance of both Kolmogorov and the proposed Gaussian spectra under identical conditions of simulation, IM/DD links are assumed operating through a 250 m horizontal path at a bit rate of 50 Mbps and transmitting pulses with on-off keying (OOK) formats under the assumption of equivalent bandwidth of 50 MHz. The criterion of constant average optical power is adopted, being one of the most important features of IM/DD channels (Jurado-Navas et al., 2010). In relation to the detection procedure, a maximum likelihood (ML) detection and a soft-decision decoding are considered respectively. A 830-nm laser wavelength is employed. All these features are included in the system model proposed in Figure 5 so that the spectra under study (Kolgomorov and Gaussian) can be compared under identical conditions of simulation. Thus its remarkable elements are: first, the channel model depicted in this chapter corresponding to a turbulent atmospheric environment, where the component of the wind velocity transverse to the propagation direction, $u_\perp$ is taken to be 8 m/s. This average wind velocity is a typical magnitude, at least in southern Europe being the main reason to employ this concrete magnitude. On the other hand, the values of turbulence strength structure parameter, C_n^2 were set to 1.23×10^{-14} and 1.23×10^{-13} $\mathrm{m}^{-2/3}$ for $\sigma_\chi^2 = 0.01$ and 0.1, respectively and for plane waves. As a second remarkable element of Figure 5, a three-pole Bessel high-pass filter with a -1 dB cut-off frequency of 500 kHz for natural (solar) light suppression is designed. However, this is an optional stage that can be

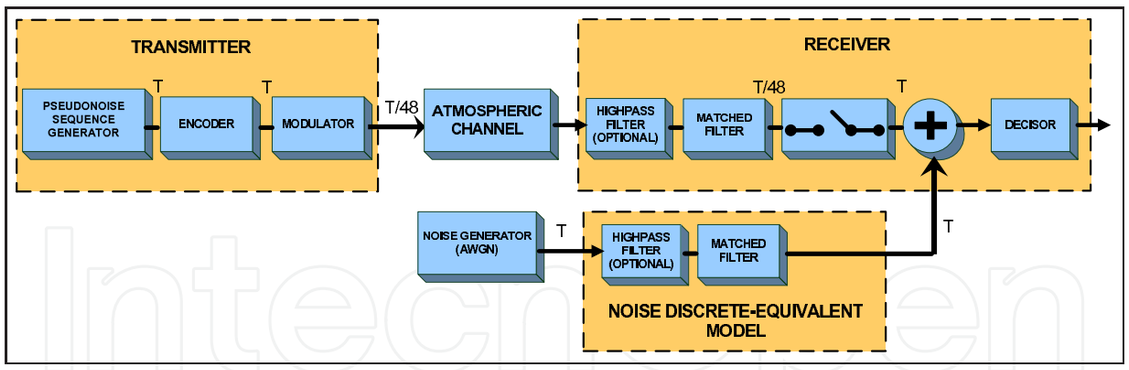

Fig. 5. Atmospheric optical system model with Monte-Carlo bit error rate estimation.

suppressed. Finally, a five-pole Bessel low-pass filter employed as a matched filter constitutes the third main stage of Figure 5. The receivers employed here are point receivers whereas the weather-induced attenuation is neglected so that we concentrate our attention on turbulence effects. Furthermore, the atmospheric-induced beam spreading that causes a power reduction at the receiver is also neglected because we are considering a terrestrial link where beam divergence is typically on the order of 10 μRad.

As a remarkable comment, with the inclusion of a wind speed, concretely 8 m/s as was said before, we can study the effect of the channel coherence in terms of burst error rate (Jurado-Navas et al., 2007) so that we obtain highly reliable link performance predictions. In addition, in urban atmospheres, especially near or among roughness elements, strong wind shear is expected to create high turbulent kinetic energy, as was detailed in (Christen et al., 2007). In such assumptions, we could have employed a higher magnitude for the wind speed without loss of generality. This fact even avoids a higher numerical complexity when we generate the lognormal scintillation sequence. Finally, and for simplicity, we assume that the wind direction is entirely transverse to the path of propagation. For special scenarios where Taylor's hypothesis may not be fully satisfied (scenarios affected by strong wind shear, urban environments or tropical areas), the procedure needed to generate the scintillation pattern may be modified as detailed in (Jurado-Navas & Puerta-Notario, 2009). In such cases, scintillation sequences registered by a receiver will not be identical to the patterns seen by another receiver except for a small shift in time, but the entrance of new structures into the optical propagation path may introduce new fluctuations into the received irradiance. Although Taylor's hypothesis is a good estimate for many cases, and for mathematical convenience this Taylor's hypothesis is assumed to be fully satisfied in this paper, however, the corrections proposed in (Jurado-Navas & Puerta-Notario, 2009) may be very useful to obtain more realistic results in particular environments.

The obtained performance for an OOK format with a 25% duty cycle are presented in terms of burst error rate average, as displayed in Figure 6 (Jurado-Navas et al., 2007). Hence, the impact of the atmospheric channel coherence on the behavior of the different signalling schemes can be taking into account, as was indicated in (Jurado-Navas et al., 2007), due to burst error rate average represents a second order of statistics and so, the temporal variability of the received irradiance fluctuations can influence on such metric of performance. However, this fact is not considered simply by doing a bit error rate analysis since bit error rate does not change with the variable wind speed, i.e., bit error rate is the first order of statistics and, consequently, it is just a function of the lognormal channel variance. Accordingly such bursts of errors are affected by the temporal duration of the turbulence-induced fadings, as it was already contemplated in Eq. (48), that was depending on τ_0 and consequently, from Eq. (42),

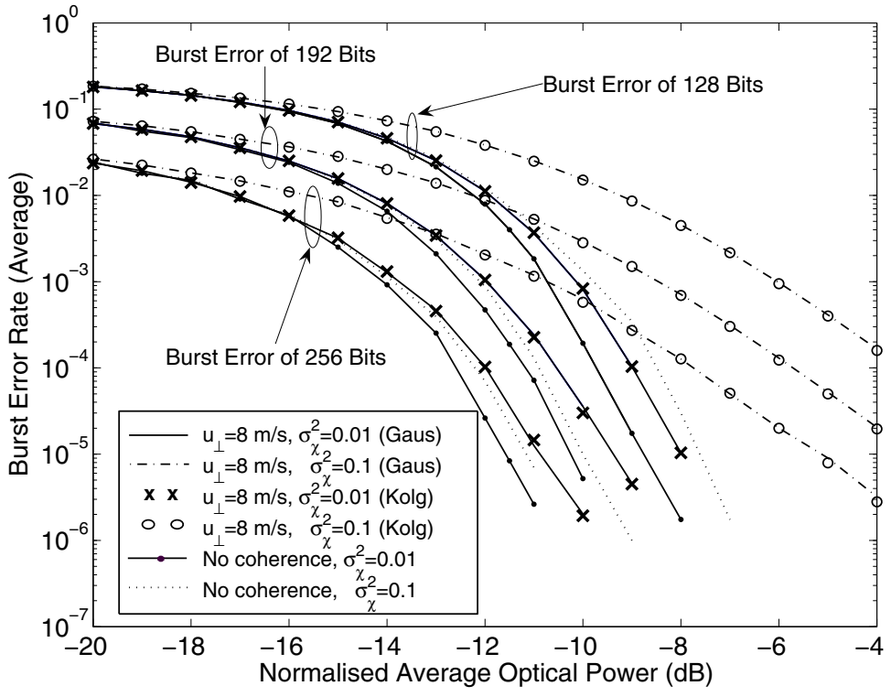

Fig. 6. Burst error rate against normalized average optical power for OOK format with a 25 % duty cycle for $\sigma_\chi^2 = 0.1$ and 0.01 and for $u_\perp = 8$ m/s and no coherence ($u_\perp \to \infty$). The burst error length is established to 256, 192 and 128 bits (Jurado-Navas et al., 2007).

in inverse proportion to $u_\perp$. Concretely, two time-varying scintillation sequences, $\alpha_{sc}(t)$ are represented in Figure 7 for two different average wind speed transverse to the direction of propagation. Hence, different temporal variabilities in such scintillation sequences must entail different performance in any atmospheric optical link.

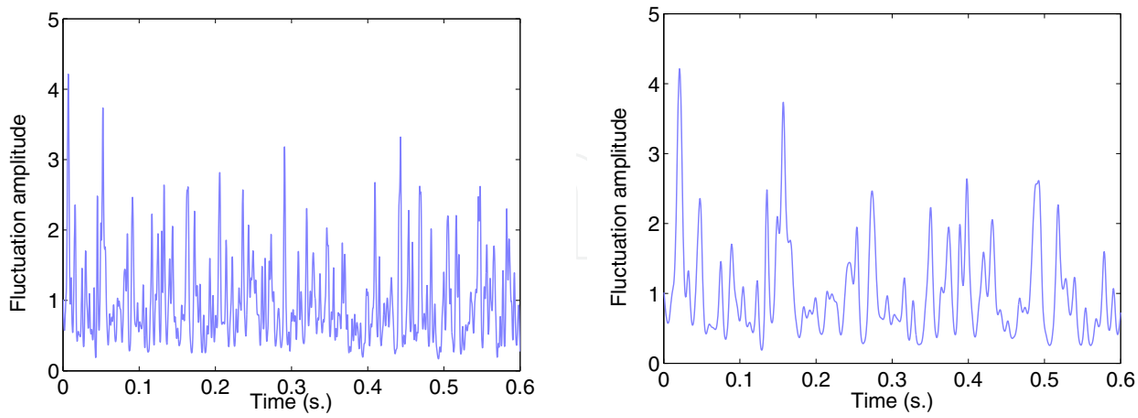

Fig. 7. Time-varying atmospheric scintillation sequence, $\alpha_{sc}(t)$ generated for an average wind speed transverse to the direction of propagation of a) $u_\perp$ = 8 m/s. b) $u_\perp$ = 2.5 m/s.

To include these atmospheric coherence effects, we followed Deutsch and Miller's (Deutsch & Miller, 1981) definition of a burst error with lengths of 256, 192 and 128 bits

respectively for the particular case of Figure 6, not containing more than $L_b - 1$ consecutive correct bits ($L_b = 5$ as explained in (Deutsch & Miller, 1981)) any sequence of burst error. An excellent agreement between our proposed channel model and the theoretical model can be observed from the results included in such a figure.
Additionally, the main conclusion we can deduce from Figure 7 is the vulnerability to the coherence of the channel in FSO communications, specially if the variance of the log-amplitude of the intensity, σ_χ^2, increases. Thus, for instance, if comparing both the curves where channel coherence has been taking into account to the ideal curves without the adverse effect of the coherence, we can achieve a cut in average optical power requirements above 0.8 and 5.9 optical dB at a burst error rate of 10^{-5} for $\sigma_\chi^2 = 0.01$ and 0.1, respectively, assuming a burst error with length of 256 bits. In this sense, the consideration of the atmospheric coherence may be a key factor to value a much more realistic performance of these systems in order to obtain a more detailed information about the design of a specific FSO link.
A wide set of results can be consulted in (Jurado-Navas et al., 2010) for different transmission schemes including repetition coding, pulse-position modulation (PPM) or even an alternative rate-adaptive transmission techniques based on the use of variable silence periods and on-off keying (OOK) formats with memory.

7. Conclusion

In this chapter, we have presented a novel easily implementable model of turbulent atmospheric channel in which the adverse effect of the turbulence on the transmitted optical signal is included. We adopt some of the ideas proposed in (Brookner, 1970) that represent the starting point for our investigation. Thus a locally homogeneous and locally isotropic atmosphere is supposed through which a plane wave is transmitted under a weak fluctuation regime. Under these assumptions, a time-varying atmospheric scintillation sequence is generated and included in a multiplicative model. Some useful techniques have also been employed to reduce the computational load: so, first, to generate the sequence of scintillation coefficients, it has been chosen to adapt to optical environments the Clarke's method, so frequently used in fading channels in radiofrequency. It consists on filtering a random statistically Gaussian signal. Hence, the output signal, i.e. $\chi(t)$, keeps on being statistically Gaussian, but shaped in its power spectral density by the filter, $H_{sc}(f)$, employed in this method. This $H_{sc}(f)$ filter is forced to have a linear phase to minimize any effect on the modulus of the filter. Second, the continuous-time signal of the filter is sampled, converting it in a discrete time signal because of their advantages in realizations. In this respect, we initially select a very low sampling rate, F_s, to obtain a first and decimated version of the atmospheric scintillation sequence. This fact let the computation time be remarkably reduced. The election of the F_s magnitude must satisfy the Nyquist sampling theorem and should help avoid aliasing, should improve resolution and should reduce noise, removing the possibility of obtaining a very oversampled signal with very few useful samples of information. At the end of the process, the scintillation sequence will be interpolated later up to a much higher sample rate, which provides it with the adequate temporal variability.
As a third useful technique employed to reduce the computational load, the $H_{sc}(f)$ filter is proposed to be as a causal FIR filter. For this purpose, a window method is considered, employing a Hamming window owing to it is optimized to minimize the maximum side lobe. Then, a zero-padding process to compute a linear convolution by a circular convolution avoiding time-aliasing is implemented. A fast Fourier algorithm is employed to compute all values of the DFTs so that the number of arithmetical operations required will be substantially

reduced. In this respect, the number of samples of any FFT is a power of two. Thus the well-known decimation-in-time radix-2 Cooley-Tukey algorithm is implemented.
However, the most important decision taken to reduce the computational load is the proposal of a second-order Gaussian statistical model that substitutes the theoretical Kolmogorov spectrum, offering a great analytical simplicity. The integration time involved in such process is reduced 12-15 times in a DELL computer (8 Gb RAM, 8 CPU processors at 2.66 GHz each one).
On another note, the model shown in (Gujar & Kavanagh, 1968) is taken into account. Hence it makes the statistical conversion from Gaussian to the desired statistical nature (lognormal, gamma-gamma, Beckmann, etc.) much easier and better modularized in structure due to its well differentiated stages.
Finally, we must remark that a great accuracy in results using the approximation proposed in Eq. (46) instead of the theoretical model is achieved and, secondly, we have demonstrated the need to include consideration of channel coherence as a key factor to fully evaluate the performance of atmospheric optical communication systems.

8. Acknowledgment

This work was supported by the Spanish Ministerio de Ciencia e Innovación, Project TEC2008-06598.

9. Nomenclature

$B_I(\tau)$, $B_\chi(\tau)$	Covariance function of irradiance and log-amplitude, respectively.
C_n^2	Refractive-index structure parameter.
$D_n(r)$	Index of refraction structure function.
d_0	Correlation length of intensity fluctuations.
$\mathbf{E}$	Vector amplitude of the electric field.
f_c	Power spectral density bandwidth of the intensity fluctuations.
$f_\chi(\chi)$	Probability density function of random log-amplitude scintillation.
$f_I(I)$	Probability density function of intensity fluctuations (=$f_{\alpha_{sc}}(\alpha_{sc})$).
${}_1F_1(a;c;v)$	Confluent hypergeometric function of the first kind.
$\mathbf{H}$	Vector amplitude of the magnetic field.
$h_{sc}(t)$	Impulse response of the filter $H_{sc}(f)$.
$h_{sc}[n]$	Discrete version of the impulse response of the filter $H_{sc}(f)$.
$h_{wsc}[n]$	$h_{sc}[n]w[n]$.
$h_{wsc;zp}[n]$	Zero pad version of $h_{wsc}[n]$.
$H_{sc}(f)$	Filter frequency response.
$H_{sc}[k]$	Discrete version of the filter frequency response.
I	Irradiance of the random field.
I_0	Level of irradiance fluctuation in the absence of air turbulence.
$J_v(\cdot)$	Bessel function of order v.
k	Wave number of beam wave (=$2\pi/\lambda$).
L	Propagation path length.
l_0	Inner scale of turbulence.
L_0	Outer scale of turbulence.
$n(\mathbf{r})$	Index of refraction.
n_0	Average value of index of refraction.

n_1	Fluctuations of the refractive index.
$p_n(t)$	Pulse shape having normalized amplitude.
$\mathbf{r}$	Transverse position of observation point.
r	Magnitude of the transverse distance between two points.
S	Random phase of the field.
$S_\chi(\omega)$	Temporal spectrum of log-amplitude perturbation.
$U_0(\mathbf{r}, z)$	Complex amplitude of the field in free space.
$U_1(\mathbf{r}, z)$, $U_2(\mathbf{r}, z)$,	First and second order perturbations of the complex amplitude of the field.
$U(\mathbf{r}, z)$	Complex amplitude of the field in random medium.
$u_\perp$	Component of the wind velocity transverse to the propagation direction.
$w[n]$	Hamming window.
$\alpha_{sc}(t)$	Time-varying atmospheric scintillation sequence.
$\chi(t)$	Log-amplitude fluctuation of scintillation.
$\chi[n]$	Discrete version of log-amplitude fluctuation of scintillation.
$\hat{\chi}[n]$	$\chi[n]$ at a lower frequency rate.
κ	Scalar spatial wave number.
λ	Wavelength.
$\Phi_n(\kappa)$	Power spectrum of refractive index.
$\psi(\mathbf{r}, L)$	Phase perturbations of Rytov approximation.
$\psi_0(\mathbf{r}, L)$	Phase of the optical wave in free-space.
$\psi_1(\mathbf{r}, L)$, $\psi_2(\mathbf{r}, L)$	First and second order phase perturbations of Rytov approximation.
σ_1^2	Rytov variance for a plane wave.
σ_I^2	Scintillation index (normalized irradiance variance).
σ_χ^2	Log-amplitude variance.
τ_0	Turbulence correlation time.
ω	Discrete frequency (in rads.).

10. References

Al Naboulsi, M. & Sizun, H. (2004). Fog Attenuation Prediction for Optical and Infrared Waves. *SPIE Optical Engineering,* Vol. 43, No. 2 (February 2004), pp. 319 – 329, ISSN 0091-3286.

Andrews, L. C. & Phillips, R. L. (1998). *Laser Beam Propagation Through Random Media*, SPIE - The International Society for Optical Engineering, ISBN 081942787x, Bellingham, Washington.

Andrews, L. C.; Phillips, R. L. & Hopen, C. Y. (2000). Aperture Averaging of Optical Scintillations: Power Fluctuations and the Temporal Spectrum. *Waves in Random Media,* Vol. 10, No. 1 (2000), pp. 53 – 70, ISSN 1745-5049.

Andrews, L. C.; Phillips, R. L. & Hopen, C. Y. (2001). *Laser Beam Scintillation with Applications*, SPIE - The International Society for Optical Engineering, ISBN 0-8194-4103-1, Bellingham, Washington.

Brookner, E. (1970). Atmosphere Propagation and Communication Channel Model for Laser Wavelengths. *IEEE Transactions on Communication Technology,* Vol. 18, No. 4 (August 1970), pp. 396 – 416, ISSN 0018-9332.

Christen, A.; van Gorsel, E. & Vogt, R. (2007). Coherent Structures in Urban Roughness Sublayer Turbulence. *International Journal of Climatology,* Vol. 27, No. 14 (November 2007), pp. 1955–1968, ISSN 1097-0088.

Clifford, S. & Strohbehn, J. W. (1970). The theory of microwave line-of-sight propagation through a turbulent atmosphere. *IEEE Transactions on Antennas and Propagation*, Vol. 18, No. 2, (March 1970), pp. 264–274, ISSN 0018-926X.

Deutsch, L. J. & Miller, R. L. (1981). Burst Statistics of Viterbi Decoding, In: *The Telecommunications and Data Acquisition Progress Report*, TDA PR 42-64 (May and June 1981), pp. 187-193, Jet Propulsion Laboratory, California Institute of Technology, Pasadena, California.

Fante, R. L. (1975). Electromagnetic Beam Propagation in Turbulent Media. *Proceedings of the IEEE*, Vol. 63, No. 12 (December 1975), pp. 1669–1692, ISSN 0018-9219.

Fried, D. L. (1966). Optical Resolution Through a Randomly Inhomogeneous Medium for Very Long and Very Short Exposures. *Journal Optical Society of America*, Vol.56, No. 10, (October 1966), pp. 1372– 1379, ISSN 0030-3941.

Fried, D.L. (1967). Aperture Averaging of Scintillation. *Journal Optical Society of America,* Vol. 57, No. 2 (February 1967), pp. 169–175, ISSN 0030-3941.

Frisch, U. (1995)*Turbulence. The legacy of A.N. Kolmogorov*, Cambridge University Press, ISBN 0-521-45103-5, Cambridge, UK.

Goldsmith, A. (2005). *Wireless Communications*. Cambridge University Press, ISBN 0-521-83716-2, New York, USA.

Gujar, U.G. & Kavanagh, R.J. (1968). Generation of Random Signals with Specified Probability Density Functions and Power Density Spectra. *IEEE Transactions on Automatic Control,* Vol. 13, No. 6 (December 1968), pp. 716 – 719, ISSN 0018-9286.

Hill, R. J. & Frehlich, R. G. (1997). Probability distribution of irradiance for the onset of strong scintillation. *Journal Optical Society America A* Vol. 14, No. 7 (July 1997), pp. 1530–1540, ISSN 0740-3232.

Huang, W.; Takayanagi, J.; Sakanaka, T. & Nakagawa, M. (1993) Atmospheric Optical Communication System using Subcarrier PSK Modulation. *IEICE Transactions on Communications,* Vol. E76-B, No. 9 (September 1993), pp. 1169 – 1176, ISSN 0916-8516.

Ishimaru, A. (1997) *Wave Propagation and Scattering in Random Media*, IEEE Press and Oxford University Press, Inc. vol. 1-2, ISBN 0-7803-4717-X, New York, USA.

Juarez, J. C.; Dwivedi, A.; Hammons, A. R.; Jones, S. D.; Weerackody, V. & Nichols, R.A. (2006). Free-Space Optical Communications for Next-Generation Military Networks. *IEEE Communications Magazine,* Vol. 44, No. 11 (November 2006), pp. 46–51, ISSN 0163-6804.

Jurado-Navas, A.; García-Zambrana, A. & Puerta-Notario A. (2007). Efficient Lognormal Channel Model for Turbulent FSO Communications. *IEE Electronics Letters,* Vol. 43, No. 3 (February 2007), pp. 178 – 180, ISSN 0013-5194.

Jurado-Navas, A. & Puerta-Notario, A. (2009). Generation of Correlated Scintillations on Atmospheric Optical Communications. *Journal of Optical Communications and Networking,* Vol. 1, No. 5 (October 2009), pp. 452–462, ISSN 1943-0620.

Jurado-Navas, A.; Garrido-Balsells, J.M..; Castillo-Vázquez, M. & Puerta-Notario A. (2009). Numerical Model for the Temporal Broadening of Optical Pulses Propagating through Weak Atmospheric Turbulence. *OSA Optics Letters,* Vol. 34, No. 23 (December 2009), pp. 3662 – 3664, ISSN 0146-9592.

Jurado-Navas, A.; Garrido-Balsells, J.M..; Castillo-Vázquez, M. & Puerta-Notario A. (2010). An Efficient Rate-Adaptive Transmission Technique using Shortened Pulses for Atmospheric Optical Communications. *OSA Optics Express*, Vol. 18, No. 16 (August 2010), pp. 17346–17363, ISSN 1094-4087.

Kennedy, R. (1968). On the Atmosphere as an Optical Communication Channel. *IEEE Transactions on Information Theory,* Vol. 14, No. 5 (September 1968), pp. 716–724, ISSN 0018-9448.

Lawrence, R. & Strohbehn, J. W. (1970). A Survey of Clear-Air Propagation Effects Relevant to Optical Communications. *Proceedings of the IEEE,* Vol. 58, No. 10 (October 1970), pp. 1523–1545, ISSN 0018-9219.

Mercier, F.P. (1962). Diffraction by a Screen Causing Large Random Phase Fluctuations. *Mathematical Proceedings of the Cambridge Philosophical Society,* Vol. 58, No. 2 (April 1962), pp. 382–400, ISSN 0305-0041.

Muhammad, S.S.; Kohldorfer, P. & Leitgeb, E. (2005). Channel Modeling for Terrestrial Free Space Optical Links. *Proceedings of 2005 7th International Conference on Transparent Optical Networks,* IEEE, Barcelona, Spain, pp. 407–410, ISBN 0-7803-9236-1.

Nugent, P. W.; Shaw, J. A. & Piazzolla, S. (2009) Infrared Cloud Imaging in Support of Earth-Space Optical Communication. *OSA Optics Express*, Vol. 17, No. 10 (May 2009), pp. 7862–7872, ISSN 1094-4087.

Oppenheim, A. V. (1999). *Discrete-Time Signal Processing* (2nd edition), Prentice-Hall, ISBN 0-13-754920-2, Upper Saddle River, New Jersey, USA.

Papoulis, A. (1991). *Probability, Random Variables, and Stochastic Processes* (3rd edition), McGraw-Hill, ISBN 0070484775, New York, USA.

Rappaport, T. S. (1996). *Wireless Communications - Principles and Practice*. Prentice Hall, ISBN 0-13-375536-3, Upper Saddle River, New Jersey, USA.

Ruike, Y.; Xiange, H; Yue, H. & Zhongyu, S. (2007). Propagation Characteristics of Infrared Pulse Waves through Windblown Sand and Dust Atmosphere. *International Journal of Infrared and Millimeter Waves*, Vol. 28, No. 2 (February 2007), pp. 181–189, ISSN 0195-9271.

Strohbehn, J.W. (1968) Line-of-Sight Wave Propagation through the Turbulent Atmosphere. *Proceedings of the IEEE*, Vol. 56, No. 8 (August 1968), pp. 1301–1318, ISSN 0018-9219.

Strohbehn, J.W. (1971) Optical Propagation through the Turbulent Atmosphere. in *Progress in Optics*, Vol. 9, pp. 73 – 122, ISBN 0720415098, edited by E. Wolf (North-Holland, Amsterdam, 1971).

Strohbehn, J.W. (1978)*Laser Beam Propagation in the Atmosphere*, Springer, Topics in Applied Physics Vol. 25, ISBN 3-540-08812-1, New York, USA.

Strohbehn, J.W. & Clifford, S.F. (1967) Polarization and Angle-of-Arrival Fluctuations for a Plane Wave Propagated through a Turbulent Medium. *IEEE Transactions on Antennas and Propagation*, Vol. 15, No. 3 , (May 1967), pp. 416–421, ISSN 0018-926X.

Tatarskii, V. I. (1971). *The Effects of the Turbulent Atmosphere on Wave Propagation*, McGraw-Hill, ISBN 0 7065 06804, New York, USA.

Taylor, G.I. (1938). The Spectrum of Turbulence. *Proceeding of the Royal Society of London. Series A, Mathematical and Physical Sciences,* Vol. 164, No. 919 (February 1938), pp. 476–490.

Young, C. Y.; Andrews, L. C. & Ishimaru, A. (1998). Time-of-Arrival Fluctuations of a Space-Time Gaussian Pulse in Weak Optical Turbulence: an Analytic Solution. *Applied Optics*, Vol. 37, No.33, (November 1998), pp. 7655-7660, ISSN 0003-6935.

Zhu, X. & Kahn, J.M. (2002). Free-space Optical Communication through Atmospheric Turbulence Channels. *IEEE Transactions on Communications*, Vol. 50, No.8, (August 2002), pp. 1293-1300, ISSN 0090-6778.

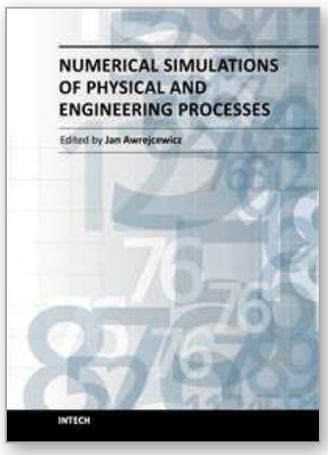

Numerical Simulations of Physical and Engineering Processes
Edited by Prof. Jan Awrejcewicz

ISBN 978-953-307-620-1
Hard cover, 594 pages
Publisher InTech
Published online 26, September, 2011
Published in print edition September, 2011

Numerical Simulations of Physical and Engineering Process is an edited book divided into two parts. Part I devoted to Physical Processes contains 14 chapters, whereas Part II titled Engineering Processes has 13 contributions. The book handles the recent research devoted to numerical simulations of physical and engineering systems. It can be treated as a bridge linking various numerical approaches of two closely inter-related branches of science, i.e. physics and engineering. Since the numerical simulations play a key role in both theoretical and application oriented research, professional reference books are highly needed by pure research scientists, applied mathematicians, engineers as well post-graduate students. In other words, it is expected that the book will serve as an effective tool in training the mentioned groups of researchers and beyond.

How to reference
In order to correctly reference this scholarly work, feel free to copy and paste the following:

Antonio Jurado-Navas, José Marîa Garrido-Balsells, Miguel Castillo-Vázquez and Antonio Puerta-Notario (2011). A Computationally Efficient Numerical Simulation for Generating Atmospheric Optical Scintillations, Numerical Simulations of Physical and Engineering Processes, Prof. Jan Awrejcewicz (Ed.), ISBN: 978-953-307-620-1, InTech, Available from: http://www.intechopen.com/books/numerical-simulations-of-physical-and-engineering-processes/a-computationally-efficient-numerical-simulation-for-generating-atmospheric-optical-scintillations

INTECH
open science | open minds

InTech Europe
University Campus STeP Ri
Slavka Krautzeka 83/A
51000 Rijeka, Croatia
Phone: +385 (51) 770 447
Fax: +385 (51) 686 166
www.intechopen.com

InTech China
Unit 405, Office Block, Hotel Equatorial Shanghai
No.65, Yan An Road (West), Shanghai, 200040, China
中国上海市延安西路65号上海国际贵都大饭店办公楼405单元
Phone: +86-21-62489820
Fax: +86-21-62489821

IntechOpen